Spatio-Temporal Modeling for fMRI Data

Wenjie Chen, Haipeng Shen, and Young K. Truong

Abstract Functional magnetic resonance imaging (fMRI) uses fast MRI techniques to enable studies of dynamic physiological processes at a time scale of seconds. This can be used for spatially localizing dynamic processes in the brain, such as neuronal activity. However, to achieve this we need to be able to infer on models of four-dimensional data. Predominantly, for statistical and computational simplicity, analysis of fMRI data is performed in two-stages. Firstly, the purely temporal nature of the fMRI data is modeled at each voxel independently, before considering spatial modeling on summary statistics from the purely temporal analysis. Clearly, it would be preferable to incorporate the spatial and temporal modeling into one all encompassing model. This would allow for correct propagation of uncertainty between temporal and spatial model parameters. In this paper, the strengths and the weaknesses of currently available methods will be discussed based on hemodynamic response (HRF) signal modeling and spatio-temporal noise modeling. Specific application to a medical study will also be described.

1 Introduction

Functional magnetic resonance imaging (fMRI) is based on the *blood-oxygen level dependent* (BOLD) principle. When neurons are active they consume oxygen, which then leads to increased blood flow to the activated area. As a result, neural activities can be inferred from the BOLD signals. In fact, the BOLD signal

Research supported by NSF DMS 1106962.

W. Chen (✉)
American Insurance Group, Inc., New York, NY, USA

H. Shen
Department of Statistics and Operations Research, University of North Carolina, Chapel Hill, NC 27599, USA

Y.K. Truong
Department of Biostatistics, The University of North Carolina, Chapel Hill, NC 27599, USA

I. Rojas, H. Pomares (eds.), *Time Series Analysis and Forecasting*, Contributions to Statistics, DOI 10.1007/978-3-319-28725-6_22

from fMRI scanner has been shown to be closely linked to neural activity [11]. Through a process called the hemodynamic response, blood releases oxygen to active neurons at a greater rate than to inactive ones. The difference in magnetic susceptibility between oxyhemoglobin and deoxyhemoglobin, and thus oxygenated or deoxygenated blood, leads to magnetic signal variation which can be detected using an MRI scanner. The relationship between the experimental stimulus and the BOLD signal involves the *hemodynamic response function* (HRF). For the simplicity of illustration, we denote the relationship by

$$\text{BOLD} = F(\text{STIMULUS}, \text{HRF}) + \text{NOISE}.$$

Several pioneer papers have used experiments to confirm that the functional form of F is approximately linear based on some typical STIMULUS such as auditory or finger tapping. Furthermore, it has been reported that the fMRI time series is hampered by the hemodynamic distortion. These effects result from the fact that the fMRI signal is only a secondary consequence of the neuronal activity. See, for example, Glover [8]. These observations have simplified the above model greatly leading to the following popular model adopted by many fMRI studies:

$$\text{BOLD} = \text{convolution}(\text{STIMULUS}, \text{HRF}) + \text{NOISE}. \tag{1}$$

Estimating or determining the HRF is important for the correct interpretation of neural science and human brain research. For example, standard fMRI analysis packages such as *Statistical Parametric Map* (SPM) [7] and *FMRIB Software Library* (FSL) [9] developed statistical inference based on

$$\text{BOLD} = \beta \times \text{convolution}(\text{STIMULUS}, \text{HRF}) + \text{NOISE}. \tag{2}$$

by estimating the parameter β under the following assumptions:

1. The HRF takes a pre-specified function known as the double-gamma function in the literature [8]:

$$\begin{aligned} \text{HRF}(t) &= c_1 t^{n_1} \exp(-t/t_1) - a_2 c_2 t^{n_2} \exp(-t/t_2), \\ c_i &= \max(t^{n_i} \exp(-t/t_i)), \quad i = 1, 2. \end{aligned}$$

2. The noise takes on simple time series models such as AR(1).

Some of the earlier papers also reported that the HRF may vary according to the location of the neurons and the type of stimulus [2, 4]. For example, the parameters n_i and t_i depend on the motor or auditory regions of the brain. Thus flexible nonparametric estimation of HRF is an important problem in fMRI that allows different HRFs for different subjects and different brain regions. The identification of the HRF has been studied under event-related designs because the design

paradigm allows the HRF to return to baseline or recover after every trial. Most of the approaches are time domain based because of the spiking nature of the stimuli.

In this paper, we introduce a Fourier method based on the transfer function estimate (TFE). This is a frequency domain nonparametric method for extracting the HRF from any kind of experimental designs, either block or event-related. This approach also allows TFE to detect the activation through test of hypotheses. Moreover, it can be further developed to validate the linearity assumption. This is very important as reported in some of the earlier papers, the BOLD response is an approximate linear function of the stimuli and the HRF, and the linearity assumption may not hold throughout the brain. These desirable features of TFE will be demonstrated using on simulation and real data analysis. More specifically,

- We first extend Bai et al.'s [1] method to multivariate form to estimate multiple HRFs simultaneously using ordinary least square (OLS). We also verified and reported the consistency and asymptotic normality of the OLS estimator.
- TFE detects the brain activation while estimating HRF by providing the F map and also tests the linearity assumption inherited from the convolution model.
- TFE is able to compare the difference among multiple HRFs in the experiment design.
- TFE adapts to all kinds of experiment designs, and it does not depend on the pre-specified HRF length support.

The present paper is based on the first author's Ph.D. dissertation [5] in which the methodology and its statistical sampling properties are described in more details. The current approach is based on the OLS method, a weighted least square (WLS) version for estimating the HRF has been implemented and a more detailed discussion on these approaches to fMRI can be found therein.

2 Method

In this section, we will outline how we developed TFE in order to make it feasible to estimate HRF under a multi-stimulus design experiment.

Using multiple stimuli in one experiment session is in high demand as it obtains stronger response signal compared to the single stimulus design. In the view of human brain's biological process, the advantage from multiple stimuli is to avoid the refractory effect, which causes nonlinearity in the response over time [6]. Subjects are easy to get bored if only one stimulus shows repeatedly in a session. In the view of experiment design, multiple stimuli are helpful to make efficient design in a limited time that the scanner provides. Thus the change of stimulus over successive trials is beneficial for experiment design.

2.1 Model

Consider the BOLD response model given by

$$y(t) = h_1 \otimes x_1(t) + h_2 \otimes x_2(t) + \cdots + h_n \otimes x_n(t) + z(t), \quad t = 0, \ldots, T-1, \tag{3}$$

where $x_i(t)$ represents the ith stimulus function, $h_i(t)$ is the corresponding HRF, and $\otimes$ is the binary convolution operator define by $x \otimes h(t) = \sum_u x(u)h(t-u)$. We assume that the error or noise series, $z(t)$, is stationary with 0 mean and power spectrum $s_{zz}(r)$, where r is the radian frequency. Here T is the duration of the experimental trial.

To write the convolution model (3) in a matrix form, let $\mathbf{x}(t)$ be an n vector-valued series, i.e., $\mathbf{x}(t) = (x_1(t), x_2(t), \ldots, x_n(t))^\tau$. Suppose that $\mathbf{h}(u)$ is a $1 \times n$ filter given by $\mathbf{h}(u) = (h_1(u), h_2(u), \ldots, h_n(u))$. The BOLD model (3) to be considered in this paper is

$$y(t) = \sum_u \mathbf{h}(u)\mathbf{x}(t-u) + z(t). \tag{4}$$

We further assume that the HRF $\mathbf{h}(u)$ is 0 when $u < 0$ or $u > d$, where d is the length of HRF latency determined by underlying neural activity.

Let $\mathbf{H}(\cdot)$ denote the finite Fourier transform (FFT) of $\mathbf{h}(\cdot)$ given by $\mathbf{H}(r) = \sum_t \mathbf{h}(t)\exp(-\mathrm{i}rt)$. Define similarly

$$Y(r) \equiv Y^{(T)}(r) = \sum_{t=0}^{T-1} y(t)\exp(-\mathrm{i}rt), \quad \mathbf{X}(r) \equiv \mathbf{X}^{(T)}(r) = \sum_{t=0}^{T-1} \mathbf{x}(t)\exp(-\mathrm{i}rt),$$

$$Z(r) \equiv Z^{(T)}(r) = \sum_{t=0}^{T-1} z(t)\exp(-\mathrm{i}rt), \quad r \in \mathbb{R}.$$

By the properties of FFT, we have

$$Y(r) = \mathbf{H}(r)\mathbf{X}(r) + Z(r), \quad r \in \mathbb{R}.$$

If $H(\cdot)$ is smooth, then it can be estimated reasonably well by a local approximation of the above relationship. Specifically, let K be an integer with $2\pi K/T$ near radian frequency r. Suppose T is sufficiently large. From the asymptotic property of FFT.

$$Y(2\pi(K+k)/T) \doteq \mathbf{H}(r)\mathbf{X}(2\pi(K+k)/T) + Z(2\pi(K+k)/T), \quad k = 0, \pm 1, \ldots, \pm m. \tag{5}$$

Here m is an appropriate integer to be specified, which is related to the degree of smoothing the Fourier transform in estimating the spectral density function.

By applying Fourier transform, the convolution in time domain is transformed to the product in frequency domain. The product forms the linear relationship between $Y(\cdot)$ and $\mathbf{X}(\cdot)$, which makes the estimation very much similar to the typical linear regression setting. Also, applying Fourier transform is a good way to avoid estimating the autocorrelation in the time domain. When we deal with Fourier coefficients instead of time points, these coefficients are asymptotically uncorrelated at different frequencies.

2.2 OLS Estimate

Relation (5) is seen to have the form of a multiple regression relation involving complex-valued variates provided $\mathbf{H}(r)$ is smooth. In fact, according to [3], an efficient estimator is given by

$$\hat{\mathbf{H}}(r) = \hat{\mathbf{s}}_{\mathbf{yx}}(r)\hat{\mathbf{s}}_{\mathbf{xx}}(r)^{-1}, \quad r \in \mathbb{R}. \tag{6}$$

Here $\hat{\mathbf{s}}_{\mathbf{xx}}$ is a smooth or window-type estimator of the auto-spectral density function $\mathbf{s}_{\mathbf{xx}}$ of the vector-valued processes $\mathbf{x}$, and $\hat{\mathbf{s}}_{\mathbf{yx}}$ is defined similarly as a smooth estimator of the crossed-spectra $\mathbf{s}_{\mathbf{yx}}$ of the processes y and $\mathbf{x}$.

A reasonable estimator of the HRF $\mathbf{h}$ is obtained by the inverse FFT of $\hat{\mathbf{H}}$:

$$\hat{\mathbf{h}}(u) = \frac{1}{T}\sum_{t=0}^{T-1} \hat{\mathbf{H}}\left(\frac{2\pi t}{T}\right) \exp(\mathrm{i}2\pi tu/T), \quad u = 0, 1, \ldots, d. \tag{7}$$

It has been shown that $\hat{\mathbf{h}}(u)$ has attractive sampling properties that it is an asymptotically consistent and efficient estimate of $\mathbf{h}(u)$.

3 Hypothesis Testing

After introducing TFE method, this section introduces the multivariate tests for fMRI analysis.

3.1 Key Concepts

First, we introduce two key concepts [3] here to support the hypothesis testing.

Coherence is an important statistic that provides a measure of the strength of a linear time invariant relation between the series $y(t)$ and the series $\mathbf{x}(t)$, that is, it indicates whether there is a strongly linear relationship between the BOLD response

and the stimuli. From a statistical point of view, we can test the linear time invariant assumption for the convolution model; for the fMRI exploration, we can choose the voxels with significant large coherence where the BOLD series have functional response to the stimulus, and then estimate the HRF in those voxels.

Coherence is defined as

$$\left|R_{y\mathbf{x}}(r)\right|^2 = \mathbf{s}_{y\mathbf{x}}(r)\mathbf{s}_{\mathbf{xx}}(r)^{-1}\mathbf{s}_{\mathbf{x}y}(r)/s_{yy}(r). \tag{8}$$

Coherence is seen as a form of correlation coefficient, bounded by 0 and 1. The closer to 1, the stronger linear time invariant relation between $y(t)$ and $\mathbf{x}(t)$.

The second concept is *partial coherence*. If we look at the stimulus individually, it is interesting to consider the complex analogues of the partial correlations or partial coherence. The estimated *partial cross-spectrum* of $y(t)$ and $x_i(t)$ after removing the linear effects of other $x_j(t)$ is given by

$$s_{y\mathbf{x}_i\cdot\mathbf{x}_j}(r) = s_{y\mathbf{x}_i}(r) - \mathbf{s}_{y\mathbf{x}_j}(r)\mathbf{s}_{\mathbf{x}_j\mathbf{x}_j}(r)^{-1}\mathbf{s}_{\mathbf{x}_j\mathbf{x}_i}(r). \tag{9}$$

Usually the case of interest is the relationship between the response and a single stimulus after the other stimuli are accounted for, that is, x_i is the single stimulus of interest, and $\mathbf{x}_j$ is the other stimuli involved in the design paradigm.

The partial coherence of $y(t)$ and $x_i(t)$ after removing the linear effects of $\mathbf{x}_j(t)$ is given by

$$\left|R_{yx_i\cdot\mathbf{x}_j}(r)\right|^2 = \frac{s_{yx_i\cdot\mathbf{x}_j}(r)^2}{s_{yy\cdot\mathbf{x}_j}(r)s_{x_ix_i\cdot\mathbf{x}_j}(r)}. \tag{10}$$

If $n = 2$, that is, if there are two kinds of stimulus in the experiment, it can be written as

$$\left|R_{yx_i\cdot x_j}(r)\right|^2 = \frac{\left|R_{yx_i}(r) - R_{yx_j}(r)R_{x_ix_j}(r)\right|^2}{[1 - \left|R_{yx_j}(r)\right|^2][1 - \left|R_{x_ix_j}(r)\right|^2]}. \tag{11}$$

Partial coherence is especially important when we focus on a specific stimulus. Not all stimuli are considered in equal measure. Stimuli such as the heart beat and breathing, which cannot be avoided in any experiment involving humans, are of secondary concern. Furthermore, as each type of stimulus has its own characteristics, it is natural to perform an individual statistical analysis to see how each one affects the overall fMRI response.

3.2 Testing the Linearity

The linearity assumption functions as the essential basis of the convolution model. As we know, any nonlinearity in the fMRI data may be caused by the scanner system or the human physical capability such as *refractory*. Refractory effects refer to the reductions in hemodynamic amplitude after several stimuli presented. If refractory effects are present, then a linear model will overestimate the hemodynamic response to closely spaced stimuli, potentially reducing the effectiveness of experimental analyses. It is critical, therefore, to consider the evidence for and against the linearity of the fMRI hemodynamic response.

It is possible that the nonlinearity is overwhelmed during scanning. Consequently, it is crucial to make sure that the linearity assumption is acceptable. The advantage of our method is that we can first determine whether the linearity assumption is acceptable before using the convolution model for analysis.

The value of coherence, between 0 and 1, reflects the strength of the linear relation between fMRI response and the stimuli. Under certain conditions, $\hat{R}_{Y\mathbf{x}}(r)$ is asymptotically normal with mean $R_{y\mathbf{x}}(r)$ and variance proportional to constant $(1 - R^2_{y\mathbf{x}}(r))/Tb$. Moreover, if $R_{y\mathbf{x}} = 0$, then

$$F(r) = \frac{(c-n)|\hat{R}_{y\mathbf{x}}(r)|^2}{n(1-|\hat{R}_{y\mathbf{x}}(r)^2|)} \quad \sim \quad F_{2n,2(c-n)}, \tag{12}$$

where $c = bT/\gamma$ and $\gamma = \int \kappa^2$ with κ being the lag-window generator depending on the choice of window function. If the F statistic on coherence is significant, it is reasonable to accept the linearity assumption.

3.3 Testing the Effect from a Specific Stimulus

For each brain area, stimuli have varying effects. For the motor cortex in the left hemisphere, right-hand motion causes much more neural activities than left-hand motion. Partial coherence is able to distinguish between right- and left-hand effects, determine whether left-hand motion evokes neural activity, and identify which motion has greater effect. The following test is applied for these kinds of research questions.

For partial coherence, if $R_{yx_i \cdot \mathbf{x}_j} = 0$, then

$$F(r) = \frac{c'|\hat{R}_{yx_i \cdot \mathbf{x}_j}(r)|^2}{1-|\hat{R}_{yx_i \cdot \mathbf{x}_j}(r)^2|} \quad \sim \quad F_{2,2(c'-1)}, \tag{13}$$

where $c' = bT/\gamma - n + 1$ and $\gamma = \int \kappa^2$ with κ being the lag-window generator.

3.4 Detecting the Activation

The HRF in fMRI indicates the arising neural activity. If there is activation evoked by the stimulus, then the corresponding HRF cannot be ignored. If there is no HRF in a brain region, there is no going-on neuronal activity. To detect activation in the brain region is to see whether there is underlying HRF. For our frequency method, we test $\mathbf{H}(r_0) = 0$ at stimulus-related frequency r_0.

We are interested in testing the hypothesis $\mathbf{H}(r) = 0$. This is carried out by means of analogs of the statistic (8). In the case $\mathbf{H}(r) = 0$,

$$\frac{(bT/\gamma)\hat{\mathbf{H}}(r)\hat{\mathbf{s}}_{\mathbf{xx}}(r)\overline{\hat{\mathbf{H}}(r)^{\tau}}}{n\hat{s}_{zz}(r)} \tag{14}$$

is distributed asymptotically as $\mathbf{F}_{2,2(bT/\gamma-n)}$.

3.5 Testing the Difference Between HRFs

The multivariate method simplifies the functional hypothesis testing by comparing the corresponding Fourier coefficients at frequency r in order to see whether there is any discrepancy between HRF curves corresponding to different stimuli. HRFs curves are functions, but when we focus just on Fourier coefficients at frequency r, we look at a common hypothesis testing on points. To see the difference between the two HRFs, it is enough to consider the hypothesis that the two Fourier coefficients at task-related frequency r_0 are equivalent.

As we know $\mathbf{H}(\cdot)$ is the Fourier transform of $\mathbf{h}(\cdot)$. For the contrast hypothesis to compare HRF functions $\mathbf{c}^{\tau}\mathbf{h} = 0$, we have the equivalent hypothesis $\mathbf{c}^{\tau}\mathbf{H}(r) = 0$, where r is usually the task-related frequency r_0.

In OLS method, we know the distribution of $\hat{\mathbf{H}}(r)^{\tau}$ is asymptotically

$$N_n^C(\mathbf{H}(r)^{\tau}, s_{zz}(r)\mathbf{\Sigma}), \quad \mathbf{H}(r) \in \mathbb{C}^n, \tag{15}$$

where

$$\mathbf{\Sigma} = \begin{Bmatrix} (bT/\gamma)^{-1}\hat{\mathbf{s}}_{\mathbf{xx}}(r)^{-1} & r \neq 0 \mod \pi \\ (bT/\gamma - 1)^{-1}\hat{\mathbf{s}}_{\mathbf{xx}}(r)^{-1} & r = 0 \mod \pi \end{Bmatrix}.$$

$N_n^C(\cdot,\cdot)$ is the complex multivariate normal distribution for the n vector-valued random variable [3].

The contrast between different HRF estimates can be represented by $\mathbf{c}^{\tau}\hat{\mathbf{H}}(r)^{\tau}$, where $\mathbf{c} = (c_1, c_2, \ldots, c_n)^{\tau}$ which satisfies that $\sum_{i=1}^{n} c_i = 0$. For the complex number $\mathbf{c}^{\tau}\hat{\mathbf{H}}(r)^{\tau}$, the hypothesis testing can be conducted by the definition of

complex normal distribution, which converts complex normal to multivariate normal distribution.

Under the hypothesis $\mathbf{c}^\tau \mathbf{H}(r) = 0$, $(\mathbf{c} \quad \mathbf{c}) \begin{bmatrix} \text{Re}\, \hat{\mathbf{H}}(r)^\tau \\ \text{Im}\, \hat{\mathbf{H}}(r)^\tau \end{bmatrix}$, denoted by $\mathbf{c}_v^\tau \hat{\mathbf{H}}_v$, where $\mathbf{c}_v^\tau = (c_1, \ldots, c_n, c_1, \ldots, c_n)$, is distributed asymptotically as

$$N\left(0, \frac{1}{2} s_{zz}(r) \mathbf{c}_v^\tau \mathbf{\Sigma}_v \mathbf{c}_v\right). \tag{16}$$

At the same time the distribution of $\hat{s}_{zz}(r)$ is approximated by an independent

$$\frac{s_{zz}(r) \chi^2_{2(bT/\gamma - n)}}{2(bT/\gamma - n)}, \quad r \neq 0 \mod \pi. \tag{17}$$

Thus, the t statistic for the contrast between different HRF estimates is

$$\frac{\mathbf{c}_v^\tau \hat{\mathbf{H}}_v(r)^\tau}{\sqrt{\frac{2(bT/\gamma - n)}{bT/\gamma} \hat{s}_{zz}(r) \mathbf{c}_v^\tau \mathbf{\Sigma}_v^{-1} \mathbf{c}_v}} \sim t_{2(bT/\gamma - n)}, \quad r \neq 0 \mod \pi. \tag{18}$$

The contrast is highly utilized in fMRI to point out the discrepancy of responses in different conditions. In the fMRI softwares SPM and FSL, we need first to specify "conditions," which is analogous to types of stimuli here. For example, if we have two types of stimuli from the right and left hands, there are two conditions: Right and Left. Then we need to set up the contrast of conditions according to our interest. For testing whether the right hand has greater effect than the left hand, the contrast should be Right > Left, equivalent to Right − Left > 0. So we state the contrast in a vector $\mathbf{c} = (1, -1)$, 1 for the condition Right and -1 for the condition Left. After settling the contrast, SPM and FSL will continue their general linear model, using parameters to conduct the t statistic.

The hypothesis of comparing the HRF similarity here equates the contrasts in SPM and FSL. We have two types of stimuli: Right and Left. Then we have respective HRF estimates for Right and Left. To test whether Right > Left, we specify $\mathbf{c} = (1, -1)^\tau$ in $\mathbf{c}^\tau \hat{\mathbf{H}}(r)^\tau$. As the result, t statistic in (18) is used for testing their difference.

3.6 Remarks

We will make a few remarks or comments on our method in contrast with the existing methods.

1. Some popular packages [7, 9] estimate the activation based on (3) and (2) using general linear models (GLM) procedure. The model considered in SPM and FSL

is given by

$$y(t) = \beta_1 h_1 \otimes x_1(t) + \beta_2 h_2 \otimes x_2(t) + \cdots + \beta_n h_n \otimes x_n(t) + z(t), \quad t = 0, \ldots, T-1, \tag{19}$$

where the HRFs $h_1, \ldots, h_n$ are pre-specified (such as the double-gamma function described in Sect. 1) and the time series $z(t)$ is a simple AR(1) model with two parameters to be estimated. Model (19) is a linear regression model with $\boldsymbol{\beta} = (\beta_1, \ldots, \beta_n)$ as the regression parameters, and the design matrix is formed by the convolution of the stimuli $\mathbf{x}(t)$ and the double-gamma functions $\mathbf{h}(t)$. The estimates of $\beta_1, \ldots, \beta_n$ are obtained by the least squares (LS) method which may be consistent (depending on the specification of the HRF) but may not be efficient. The latter is caused by the mis-specification of the AR(1) and the standard errors (se) of the LS estimates may be large. Another challenge is to conduct the voxel-wise significant test of activation. Namely, at each voxel, the test is based on the t-statistic given by

$$t = \frac{\hat{\beta}}{\text{se}(\hat{\beta})}$$

whose p-value may be over- or under-estimated depending on whether the standard error $\text{se}(\hat{\beta})$ has been correctly estimated, which in turn depends on the specification of the model for the (noise) time series $z(t)$. This will result in a higher false-positive or false-negative rates in detecting activation. One may address the estimation of the model for $z(t)$, but this will be inefficient in fitting and testing a correct time series model at each voxel. The default setting in those packages usually starts with AR(1) at the expenses of specification error.

This problem can be remedied using the TFE approach described above. Apply the discrete Fourier transform to (3) yields two important results at once. First, the TFE of HRF is direct (without introducing the β's) and consistent estimate. Second, the FFT of the noise time series is uncorrelated (exactly independent in the Gaussian case), and consequently, the F-test (14) is consistent for testing activation. Note that our F-test is described in the frequency domain, which should not be confused with the model-based F-test in SPM or FSL described in time domain, which is easily accessible by the majority of statisticians. In the current setting, however, Fourier transformation provides a direct and highly interpretable activation detection.

2. The TFE method was thought to be only applicable to block designs with some forms of periodicity. Hence the popular event-related designs have ruled out the use of it. This is certainly not the case as one can see from [3]. The current paper demonstrates the usefulness of the TFE through simulation and real data sets taken from the above package sites for the sake of comparison. More results can be found in [5].
3. The TFE also offers a check on the linearity assumption in (3) using the F-statistics based on the coherence (12). On the other hand, the time domain method

will further need to verify the error auto-covariance structure for this step, which can be inefficient for the whole brain.
4. A key issue to be addressed in using the TFE method is the smoothing parameter in estimating various auto- and cross-spectra. Some data-adaptive procedures such as cross-validation have been investigated in [5] and the HRF shape has made such a choice less challenging.
5. When the voxel time series is non-stationary, then both time and frequency domain methods will not work that well. In that situation, one can invoke the short time (or windowed) Fourier transform method (a special case of wavelets analysis) to estimate the HRF, this will be carried out in another paper.
6. An extensive review is given in one of the chapters of Chen [5]. Here the main objective is to highlight some important contributions to the problem of HRF estimation using Fourier transform. This type of deconvolution or finite impulse response (FIR) problems has been known to the area of signal processing. The various forms of the test statistics (12), (13), however, have not been appropriately addressed. Hence the aim of the current paper is to illustrate the usefulness of the statistical inference tools offered by this important frequency domain method.

4 Simulation

The simulation study was based on a multiple stimuli experiment design and a simulated brain. The experiment in the section included two types of stimuli, called *left* and *right*. The simulated brain had 8×8 voxels, which was designed to have various brain functions in the left and right experiment design. The brain was divided into four regions: one only responded to left, one only responded to right, one can respond to both left and right, and the remaining one had no response in the experiment.

The fMRI data was simulated based on the convolution model (3): the convolution of the pre-specified left HRF $h_1(\cdot)$ and right HRF $h_2(\cdot)$, and the known experiment paradigm for left stimulus $x_1(t)$ and right stimulus $x_2(t)$. The response was given by

$$Y(t) = h_1 \otimes x_1(t) + h_2 \otimes x_2(t) + z(t), \quad t = 0, \ldots, T-1 \tag{20}$$

with $T = 600$. The noise was generated from an ARMA(2, 2):

$$z(t) - 0.8897z(t-1) + 0.4858z(t-2) = w(t) - 0.2279w(t-1) + 0.2488w(t-2),$$
$$w(t) \sim_{\text{iid}} N(0, 0.2^2), \qquad t = 0, 1, \ldots, 599.$$

The ARMA was chosen to test the strength of our method under other types of correlated structures, and the coefficients were selected to illustrate the performance of the procedure under moderate, serially correlated noise.

The illustrated experiment paradigm and the brain map are shown in Fig. 1. This was an event-related design with left and right interchanging, where the green stands for the left, and the purple stands for the right. The left and right stimuli came periodically. The stimulus-related frequency for each was $1/40$, and the overall task-related frequency for the experiment was $1/20$. The brain map shows the brain function in each region (Fig. 1b).

The first simulation was to detect the activation regions in the brain. We assumed both of the original HRFs for left and right were Glover's HRF. At the experiment frequency $1/20$, the coherence and F statistic map are shown in Fig. 2. The lighter the color is, the higher the values are. The high value of coherence in the responsive region implies a strong linear relation in the simulation. Also, the F statistic represents the strength of activation in the voxel. As expected, there were three

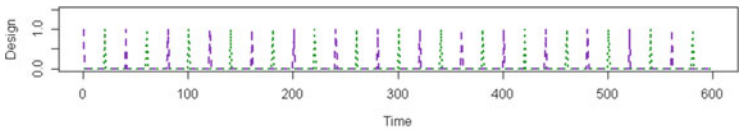

(a) Event-related design

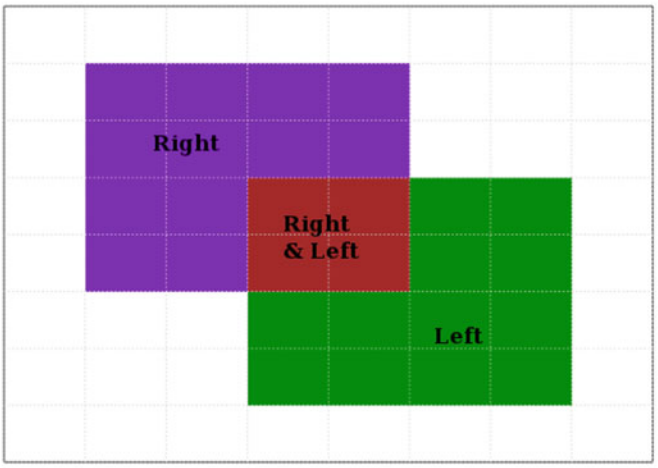

(b) Simulated brain map.

Fig. 1 The simulated brain map in the simulation. (**a**) shows the experiment design of the simulation with two kinds of stimuli, which are finger taping on the right (shown in *purple*) and on the left (shown in *green*). (**b**) is the simulated brain map: the *purple region* only responds to the right-hand stimulus; the *green region* only responds to the left-hand stimulus; the *brown region* responds to both left and right; and the *white region* has only noise. Originally published in Chen (2012). Published with the kind permission of © Wenjie Chen 2012. All Rights Reserved

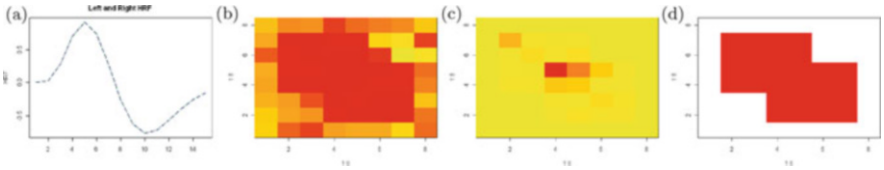

Fig. 2 Detecting the activation regions by TFE. The activation region is where the brain has response to the experiment stimulus. (**a**) shows that the true HRFs for both left and right are the same. (**b**) shows the coherence value obtained in voxels (the *red color* means high intensity, and the *yellow* indicates low intensity). (**c**) shows the corresponding F statistic, called F map. As shown in (**d**), both right and left activated regions (marked in *red*) are detected. Originally published in Chen (2012). Published with the kind permission of © Wenjie Chen 2012. All Rights Reserved

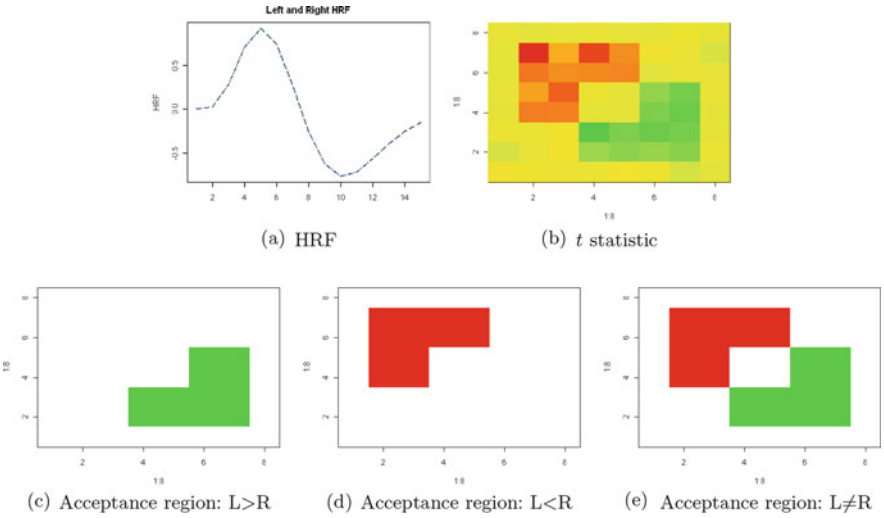

Fig. 3 Hypothesis testing with two identical HRFs in the simulated brain. (**a**) shows the Glovers HRF for both left and right. (**b**) shows the overall t statistic over the brain map, where *red color* means high positive values, *green color* means negative values, and *yellow* means near 0. (**c**) shows the rejection region for the test: left $\leq$ right; (**d**) shows the rejection region for left $\geq$ right; (**e**) shows the rejection region for left = right. Originally published in Chen (2012). Published with the kind permission of © Wenjie Chen 2012. All Rights Reserved

activation regions: Left (L), Right (R), Left and Right (L&R), which was selected at $\alpha = 0.01$ level.

At the stimulus-related frequency $1/40$ level, we compared the similarity of left and right HRFs. The true left and right HRFs are the same Glover's HRF. The HRF discrepancy region is only two regions: Left (L) and Right (R), where we regarded no response as zero HRF. The simulation result is displayed in Fig. 3. The rejection region for L>R is the region L; the rejection region for L<R is the region R; the rejection region for L≠R is L&R at level $\alpha = 0.05$. As we can see, if the voxel has the same response to different stimuli, it shows in the result that there is no difference in the HRFs.

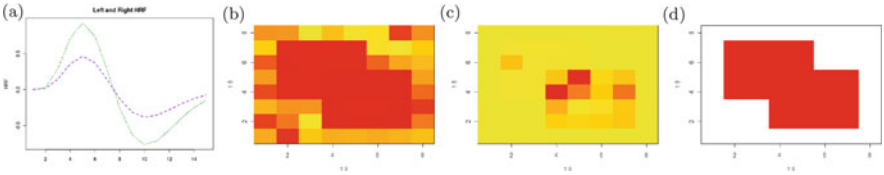

Fig. 4 Detecting the activation regions by TFE with non-identical HRFs. The activation region is where the brain has response to the experiment stimulus. (**a**) shows the true HRFs for both left (*green*) and right (*purple*). (**b**) shows the coherence obtained in voxels (the *red color* means high intensity, and the *yellow* indicates low intensity). (**c**) shows the corresponding F statistic, F map. As shown in (**d**), both right and left activated regions (marked in *red*) are detected. Originally published in Chen (2012). Published with the kind permission of © Wenjie Chen 2012. All Rights Reserved

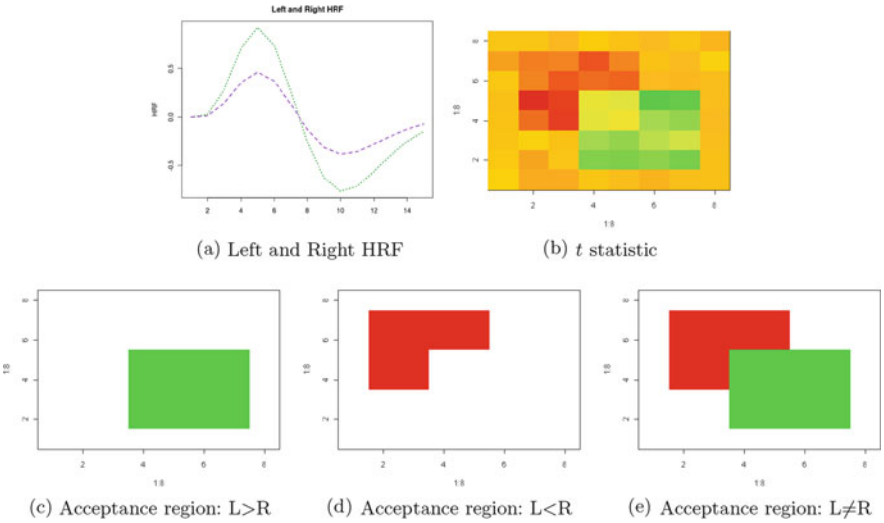

Fig. 5 Hypothesis testing with two non-identical HRFs in the simulated brain. (**a**) shows the Glovers HRF for left (*green*) and half Glovers HRF for right (*purple*). (**b**) shows the overall t statistic over the brain map, where *red color* means high positive values, *green color* means negative values, and *yellow* means near 0. (**c**) shows the rejection region for the test: left $\leq$ right; as the left HRF has much higher amplitude than the right one, the rejection region for the test left $\leq$ right is the two regions that response to left-hand stimulus. (**d**) shows the rejection region for right $\geq$ left; (**e**) shows the rejection region for left = right. Originally published in Chen (2012). Published with the kind permission of © Wenjie Chen 2012. All Rights Reserved

The second simulation was built on different HRFs. The left HRF kept Glover's HRF, and the right HRF reduced Glover's HRF to half. As we can see, the left and right HRFs had different amplitudes. The left was larger than the right one. At the experiment frequency $1/20$, the activation region is accurately spotted in Fig. 4.

At the individual-stimulus-related frequency $1/40$, the difference between left and right HRF was detected, as shown in Fig. 5. The rejection region for L>R contains the regions that respond to both L and R. The hypothesis testing of similar HRFs clearly separated different HRFs.

5 Real Data Analysis

5.1 Auditory Data

In order to test whether the method of Bai et al. [1] is applicable to real data and detect fMRI activation, we applied the nonparametric method to the published auditory data set on the Statistical Parametric Mapping website (http://www.fil.ion.ucl.ac.uk/spm/data/auditory/). According to the information listed on the website, these whole brain BOLD/EPI images were acquired on a modified 2T Siemens MAGNETOM Vision system. Each acquisition consisted of 64 contiguous slices ($64 \times 64 \times 64$, 3 mm $\times$ 3 mm $\times$ 3 mmvoxels). Acquisition took 6.05 s, with the scan to scan repeat time (TR) set arbitrarily to 7 s. During the experiment 96 acquisitions were made in blocks of 6 that resulted in 16 42-s blocks. The blocks alternated between rest and the auditory stimulation. We included eight trials in our dataset, with the first six images acquired in the first run discarded due to T1 effects. The data was preprocessed using SPM5, and included realignment, slice timing correction, coregistration, and spatial smoothing.

Figure 6a shows the time course data from the one voxel that had the greatest F value in Eq. (14). The voxel time series depicted in Fig. 6a has been detrended [10] because the trends may result in false-positive activations if they are not accounted for in the model. Since the voxel has a high F value, its time series has good relationship to the task, similar to the pattern we obtained in our second simulation. Figure 6b shows several HRF estimates from the 12 voxels with the highest F-values in the brain. The majority of the HRF estimates closely match the HRF shape, showing the increase in the signal that corresponds to the HRF peak and some even depicting the post-dip after the peak signal. The TR for this dataset is 7 s, which corresponds to the time interval between the acquisition of data points. This

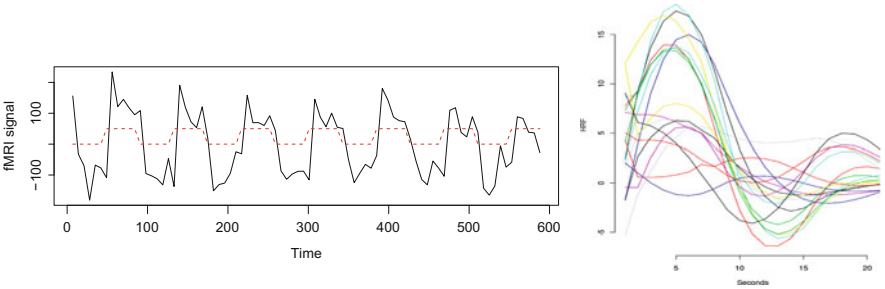

(a) Raw FMRI data from the voxel with the grea test F value (b) HRF estimates

Fig. 6 HRF estimation for auditory data. (**a**) is the experimental design paradigm (the *red dashed line*) for the auditory data. The *solid line* is fMRI response from an activated voxel over time; (**b**) is the HRF estimates from the 12 highly activated voxels found by using TFE in the brain. Due to the large TR (7 s), there is a limitation on showing the HRF estimate in finer temporal resolution. In (**b**), we still can see the different shapes of HRF. Originally published in Chen (2012). Published with the kind permission of © Wenjie Chen 2012. All Rights Reserved

leads to a very low temporal resolution with which to measure the hemodynamic response. The limitation of large TR time for estimating HRF is not only the low temporal resolution, but it also conducts the wrong timing for the stimulus onset. For instance, if TR is seven seconds, we have 40-s blocks instead of 42-s. If the stimulus function $X(t)$ is 0–1 function which indicates the onset for every seven seconds, then we will miss the exact onset on 40, 80, 120, 160, ... s. The strategy here we used is interpolation. We interpreted the preprocessed data on the second-based time series, and then applied TFE to see the HRF. As a result, we could only see the framework of the HRF and approximate its value. Despite this limitation, the resulting framework gave us evidence that our method does indeed capture the various HRFs in the voxels. In addition, it establishes that our HRF-based analysis can be applied to real data and may be improved with correspondingly refined temporal resolution.

In the experimental design of this study, there are seven stimulus blocks in the time series data that have a total duration of 90 acquisitions. As a result, the task-related frequency is $7/90 = 0.0778$. Using this information, we can apply our method in order to generate an F-statistic map to show the activation in the brain that is triggered by the stimuli (bottom row in Fig. 7). For comparison, we also generated a T map using SPM5 (the SPM T map) that is shown in the upper row of Fig. 7. The SPM T map is a contrast image that obtains the activation triggered by the stimulus by applying the canonical SPM HRF uniformly throughout the brain. As a result, it does not take into account any HRF variation that might occur in the different regions of the brain.

In both rows of Fig. 7, increased activation is depicted by increased hot color, such that the bright yellow regions represent more activation. As expected from an auditory study, both the F map generated using our method and the SPM-generated T map display activation in the temporal lobe. The F map from our analysis shows

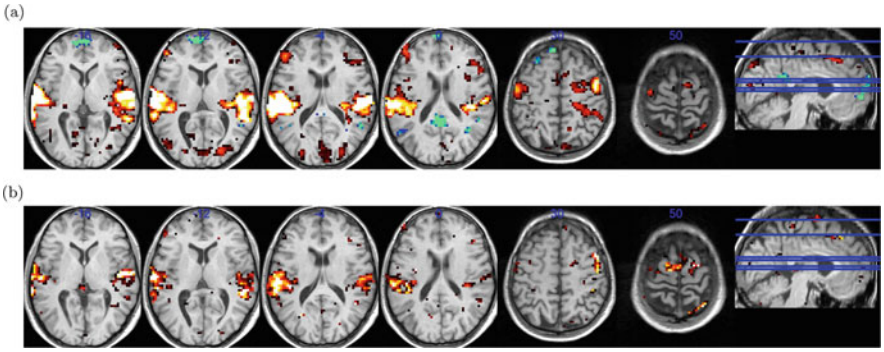

Fig. 7 (**b**) F map and (**a**) T map of the activation by using TFE and SPM. T maps contain *blue* and *hot colors* which respectively indicates negative and positive factor. The F map generated by TFE (*bottom row*) appears to have less noise compared to the SPM-generated T map (*upper row*). Originally published in Chen (2012). Published with the kind permission of © Wenjie Chen 2012. All Rights Reserved

increased activation almost exclusively in the temporal lobe, again as would be expected from an auditory study. Whereas the contrast map generated using SPM also displays the activation in the temporal lobe, there is also significant activation in other regions of the brain, including parietal and prefrontal cortical areas. In addition, the activation in the temporal lobe is more diffuse using SPM compared to that seen using our F method. We conclude that the map generated using our method appears to display less noise, such that there is less activation in regions other than the primary auditory cortex. In addition, our method displayed a less diffuse activation area in the auditory region, which may be interpreted as either a more focused activation pattern or there may be some loss of sensitivity for detecting the actual activation. Despite this possible limitation associated with our method, it does have the additional benefit of being a test for the linearity assumption.

6 Discussion

The TFE, based on the method of Bai et al. [1], completes the fMRI data analysis procedure: from adapting to various experimental design, through estimating HRF, to detecting the activation region.

The first benefit is the experiment design. TFE can be applied for any type of experimental design, including multiple stimulus design, event-related design, and block design. Our nonparametric method can be applied to the multiple stimulus experiment paradigm. From the property of HRF, different stimuli may cause different hemodynamic responses even in one specific region. Consequently, the corresponding HRF estimates to each stimulus will be given in our method, and furthermore we carry out the statistical testing to see whether they are equivalent to each other.

Our method can also be applied to block design and some rapid event-related design. Most of the existing HRF estimation methods are only applied to event-related design. With our method's adaptability to various experimental design, we extended the application to rapid event-related design and to block design by adding an extra rest period. In fact, as long as there is a resting period during the design, our method is better in estimating HRF.

The second benefit is reducing the noise. Noises might come from multiple sources, such as the various types of scanners with systematic errors in use, the background noise in the environment, and differences in the individual subjects' heart beats and breathing. These noises would lead to heterogeneity of the records of fMRI data. By using TFE, the heterogeneity is considered in the frequency domain, which simplifies the error structure estimation process. Such simplicity comes from the asymptotic independence of the spectrum in different Fourier frequencies when we transfer the time series analysis to the frequency domain. In addition, for efficiency, we use the WLS method to estimate the error spectrum. Unlike the existing work [3, 13] based on the WLS method, which is implemented by a computationally costly high-dimensional-matrix operation, our method shows

higher performance, since the dimension of our matrix operation depends only on the number of stimulus types in the experiment design.

The third benefit is HRF estimation. TFE does not require the length of HRF, which is also called the latency (width) of HRF. As in most HRF modeling methods, the length of HRF is the input as a *priori* to start the analysis. In practice, however, the latency of HRF is unknown for the researchers. If the length of HRF is assumed as known, such as in smooth FIR or the two-level method in [13], the final result may be very sensitive to the input lengths. For TFE, the latency of HRF is not a factor that affects the estimates. Additionally, the TFEs gives us a rough idea about the latency of HRF by looking at how the estimates go to zero eventually over time.

One of the most important benefits is that TFE is able to generate the brain activation map without using the general linear method (GLM). In fact, it simplified the analysis by reducing the number of steps from two to one. The typical fMRI analysis (SPM, FSL) requires two steps to customize HRF in the analysis. The first step estimates HRF, and the second step applies the GLM to study the detection of activation. Some issues related to GLM have not been addressed even in the most recent versions of these packages. For example, the estimated standard error used in tests for activation is a model-based approach and it is not efficient to check the model validity for each voxel. Nevertheless, the GLM method continue to be applied to explore other areas of brain research such as connectivity. In TFE, activation detection is generalized by testing the hypothesis for the HRF estimates, which does not require additional GLM and the specification of the error structure. Applications of TFE to Parkinson's disease and schizophrenia patients can be found in [5].

Also, the unique feature of using TFE is being able to test the linearity assumption. As the linearity assumption is the foundation of the convolution model we used, our method is able to test its validity before estimation, which is definitely important for further analysis. As the linearity assumption is valid for the fMRI data after testing, we are then able to use our nonparametric method to perform the analysis, or any analysis tool based on the linearity assumption. If the linearity testing fails, nonlinearity dominates the fMRI data, and the nonlinear estimation method might be used [6, 8, 12].

References

1. Bai, P., Huang, X., Truong, Y.K.: Nonparametric estimation of hemodynamic response function: a frequency domain approach. In: Rojo, J. (ed.) Optimality: The Third Erich L. Lehmann Symposium. IMS Lecture Notes Monograph Series, vol. 57, pp. 190–215. Institute of Mathematical Statistics, Beachwood (2009)
2. Boynton, G.M., Engel, S.A., Glover, G.H., Heeger, D.J.: Linear systems analysis of functional magnetic resonance imaging in human V1. J. Neurosci. **16**(13), 4207–4221 (1996)
3. Brillinger, D.R.: Time Series. Holden-Day, San Francisco (1981)
4. Buckner, R.L., Bandettini, P.A., OCraven, K.M., Savoy, R.L., Petersen, S.E., Raichle, M.E., Rosen, B.R.: Detection of cortical activation during averaged single trials of a cognitive task using functional magnetic resonance imaging. Proc. Natl. Acad. Sci. U. S. A. **93**(25), 14878–14883 (1996)

5. Chen, W.: On estimating hemodynamic response functions. Ph.D. thesis, The University of North Carolina at Chapel Hill (2012)
6. Friston, K.J., Josephs, O., Rees, G., Turner, R.: Nonlinear event-related responses in fMRI. Magn. Reson. Med. **39**, 41–52 (1998)
7. Friston, K.J., Ashburner, J., Kiebel, S.J., Nichols, T.E., Penny, W.D. (eds.): Statistical Parametric Mapping: The Analysis of Functional Brain Images. Academic, New York (2007). http://www.fil.ion.ucl.ac.uk/spm/
8. Glover, G.H.: Deconvolution of impulse response in event-related BOLD fMRI1. NeuroImage **9**(4), 416–429 (1999)
9. Jenkinson, M., Beckmann, C.F., Behrens, T.E., Woolrich, M.W., Smith, S.M.: Fsl. NeuroImage **62**, 782–790 (2012). http://www.fmrib.ox.ac.uk/fsl/
10. Marchini, J.L., Ripley, B.D.: A new statistical approach to detecting significant activation in functional MRI. NeuroImage **12**(4), 366–380 (2000)
11. Ogawa, S., Lee, T.M., Kay, A.R., Tank, D.W.: Brain magnetic resonance imaging with contrast dependent on blood oxygenation. Proc. Natl. Acad. Sci. U. S. A. **87**(24), 9868–9872 (1990)
12. Vazquez, A.L., Noll, D.C.: Nonlinear aspects of the BOLD response in functional MRI. NeuroImage **7**(2), 108–118 (1998)
13. Zhang, C., Jiang, Y., Yu, T.: A comparative study of one-level and two-level semiparametric estimation of hemodynamic response function for fMRI data. Stat. Med. **26**(21), 3845–3861 (2007)